AIChE

R&D NOTE

Insight into Approximations for Drug Release from Polymer Matrix

Sung-Hwa Lin
Dept. of Chemical Engineering and Materials Engineering, National Ilan University, Yilan 26047, Taiwan

DOI 10.1002/aic.11533
Published online June 10, 2008 in Wiley InterScience (www.interscience.wiley.com).

Keywords: undissolved drug, polymer matrix, heat-balance integral method, integrodifferential equation, polynomial concentration profile

Introduction

Controlled release of drug in polymer matrix is of essence in medical application of long-term effects. For long-term purpose, solid drug in polymer matrix is usually set higher in concentration than its solubility. In this condition, depending on the dissolution rate of drug, there are two major mathematical models, diffusion-controlled release and dissolution/diffusion-controlled release, where in the former, dissolution rate is much faster if compared with diffusion rate, and in the latter, these two rates are comparable. For diffusion-controlled release, because of the presence of undissolved drug, two distinct zones, separated by moving saturation front, appear, and mathematical complexity arises. Analytical solutions for this kind of moving boundary problem, as well as its analog in heat conduction, i.e. Stefan's problem or freezing and melting problem, are limited,[1,2] and resort to approximate or numerical approach is requisite in general. In literature, important approximate methods applicable to this kind of problem include pseudosteady state approximation,[3] heat-balance integral method,[4–7] a refinement of integral method by Volkov and Li-Orlov,[8,9] and finite integral transform.[10] Numerical methods include graphical method or method of series of fixed boundaries,[11] Landau transform,[12] moving grid method,[13] and finite element method.[14] In approximate methods mentioned earlier, the first three can be classified into integral method. The integral method originates in boundary-layer theory.[15] For boundary-layer in laminar flow regime, some simple and regular problems have similar solutions, that is, all velocity profiles inside layer belong to one profile family. And in this situation, analytically exact solutions for boundary layer are available. If it is not the case, boundary-layer problem can be approximated by integral method. An important approximation in integral method is that, all velocity profiles inside layer are assumed to come from one approximate profile family. Based on this approximation, using approximate velocity profile in integral equation, approximations for important parameters in boundary-layer, such as boundary-layer thickness, displacement thickness, momentum thickness, and wall shear stress, can be restored. In the first integral method ever used, the famous Karman-Pohlhausen method, a polynomial velocity profile of degree four was applied in momentum integral equation. For mathematical similarity between boundary-layer problem and heat-conduction problem, Goodman proposed the heat-balance integral method, which is quite similar to Karman-Pohlhausen method, for solving transient heat conduction problems concerning infinite slab,[4,6] phase of change,[4,6] variable thermal properties,[5,6] and so forth. The pseudosteady state approximation, used by Higuchi,[3] is covered by heat-balance integral method, where linear polynomial concentration profile is introduced in integral equation. Langford[7] analyzed accuracy of heat-balance integral method using miscellaneous temperature profiles satisfying different sets of boundary or subsidiary conditions. In all of polynomial profiles of degree up to four used in his work, the result using polynomial profile of degree four appears the most satisfactory; however, accuracy of approximation is found not always improved by increasing degree of polynomial profile. A refinement of integral method is proposed by Volkov and Li-Orlov[8] in heat-conduction problem. For possibility of marked error in the derivative term in integral equation in heat-balance integral method if approximate profile is introduced, they suggested a double-integration technique to eliminate the derivative term. A substitutive integral equation, called integrodifferential equation, was arrived at, and

Correspondence concerning this article should be addressed to S. H. Lin at shlin@niu.edu.tw.

accuracy of result, using this integral equation, was found improved significantly, especially for heat-conduction problems concerning variable thermal properties.

Analytically approximate solution is always of interest and of value. In this contribution, an attempt is made on assessment of applicability of integral methods for diffusion-controlled release for drug dispersed excessively in polymer matrix, The classical release problem discussed by Higuchi[3] is under consideration here. There are two reasons for this. First, this classical problem has analytically exact solution. Second, in this classical model, there is only one key parameter, i.e. quantity of undissolved drug. Both of these two reasons benefit the analyses. In addition to these two integral methods mentioned earlier, an approximate method is also considered for comparison. All possible polynomial concentration profiles will be taken into account for each approximate method to evaluate these approximate methods.

Mathematical Model and Exact Solution

The classical release model, considered by Higuchi,[3] for drug release from a thin, planner polymer matrix into a well-stirred reservoir is demonstrated in Figure 1. The drug is initially loaded in polymer matrix in excess of drug solubility c_s, and undissolved drug is c_u in quantity per unit volume. Therefore, the total quantity of drug in unit volume is $c_s + c_u$. The thickness of polymer matrix is $2l_p$, where l_p is the distance between central symmetric plane of polymer matrix and polymer matrix/reservoir interface. Relevant assumptions are summarized as follows:

(1) The polymer matrix/reservoir interface is assumed to be much greater in scale than the thickness of polymer matrix, and hence, release model can be reduced into an one-dimensional problem.

(2) The reservoir is assumed to be large compared with scale of polymer matrix, i.e. a perfect sink.

(3) The dissolution rate of the drug is much greater than the diffusion rate of drug.

The abscissa x originates from interface and extends into the polymer matrix. Hence, position of central symmetrical plane is at $x = l_p$. Based on the third assumption, polymer matrix is divided into two distinct zones, diffusion zone and saturation zone, by moving saturation front, of which position is denoted by $x_s(t)$, as shown in Figure 1. In diffusion zone, where $x \in [0,x_s(t)]$, drug concentration is denoted by $c(x,t)$. In saturation zone, where $x \in [x_s(t),l_p]$, drug is saturated, together with undissolved drug c_u in quantity per unit volume. Consequently, relevant mathematical equations in diffusion zone can be summarized as follows:

$$\frac{\partial C}{\partial T} - \frac{\partial^2 C}{\partial X^2} = 0 \tag{1}$$

$$\left.\frac{\partial C}{\partial X}\right|_{X=X_s} - C_u \frac{dX_s}{dT} = 0 \tag{2}$$

$$C = 0, \quad X = 0 \tag{3}$$

$$C = 1, \quad X = X_s \tag{4}$$

$$X_s = 0, \quad T = 0 \tag{5}$$

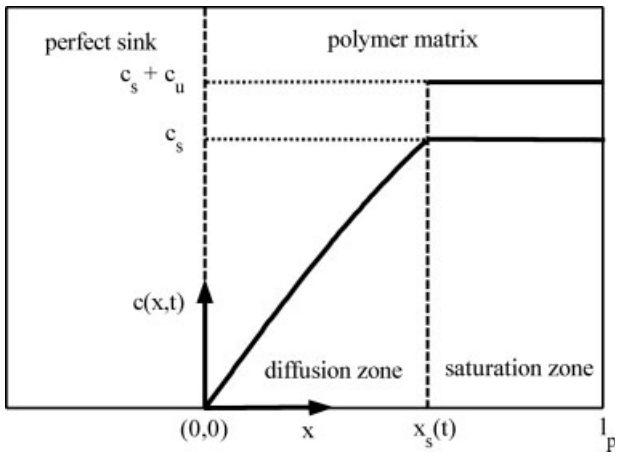

Figure 1. Schematic representation for drug release from polymer matrix.

where $C = c/c_s$, $C_u = c_u/c_s$, $X = x/l_p$, $X_s = x_s/l_p$, $T = Dt/l_p^2$, with D being the diffusivity of drug in polymer matrix. In these equations, Eq. 2 represents the temporal dependence of moving saturation front, Eqs. 3 and 4 are boundary conditions, and Eq. 5 is initial condition. Equation 3 is due to perfect sink.

The exact solutions corresponding to Eqs. 1–5 are summarized as follows[1,2]:

$$C = \frac{\operatorname{erf}(\lambda\eta)}{\operatorname{erf}(\lambda)} \tag{6}$$

$$X_s = 2\lambda T^{1/2} \tag{7}$$

$$f = \frac{2}{\pi^{1/2}(1 + C_u)\operatorname{erf}(\lambda)} T^{1/2} \tag{8}$$

$$\pi^{1/2} C_u \lambda e^{\lambda^2} \operatorname{erf}(\lambda) - 1 = 0 \tag{9}$$

where $\eta = x/x_s = X/X_s$, and f is the fraction of drug released. From overall mass balance, f can be expressed by

$$f = \frac{\int_0^{x_s} (c_s + c_u - c)\, dx}{(c_s + c_u) l_p} = \frac{\left(1 + C_u - \int_0^1 C\, d\eta\right) X_s}{1 + C_u} = 1 - \frac{\int_0^1 C\, d\eta X_s}{1 + C_u} \tag{10}$$

The parameter λ in Eqs. 6–8 is determined by C_u via Eq. 9. According to Eq. 9, we have $\lim_{C_u \to 0} \lambda \to \infty$, and $\lim_{C_u \to \infty} \lambda = 0$. Also by differentiating Eq. 9 with respect to C_u implicitly, we have

$$\frac{d\lambda}{dC_u} = -\frac{\pi \lambda^2 e^{2\lambda^2} \operatorname{erf}^2(\lambda)}{\pi^{1/2} e^{\lambda^2} \operatorname{erf}(\lambda) + 2\pi^{1/2} \lambda^2 e^{\lambda^2} \operatorname{erf}(\lambda) + 2\lambda} < 0 \tag{11}$$

Therefore, as C_u increases from 0 to infinity, λ decreases monotonically from infinity to 0.

Approximate Methods Based on Different Equations

In the following, three approximate methods, based on different equations in substitution for original diffusion equation, that is, Eq. 1, are illustrated respectively. In method I, Eq. 2 is used directly, and that is

$$\frac{dX_s}{dT} - \frac{1}{C_u}\left.\frac{\partial C}{\partial X}\right|_{X=X_s} = 0 \tag{12}$$

In method II, integral equation in Goodman's heat-balance integral method[4–6] is used. The derivation is as follows. Integration of Eq. 1 with respect to X over $[0, X_s]$, we have

$$\int_0^{X_s} \frac{\partial C}{\partial T}\, dX - \left(\left.\frac{\partial C}{\partial X}\right|_{X=X_s} - \left.\frac{\partial C}{\partial X}\right|_{X=0}\right) = 0 \tag{13}$$

Upon applying Leibnitz's rule to the first term in Eq. 13, Eq. 13 becomes

$$\frac{d}{dT}\int_0^{X_s} C\, dX - C(X_s, T)\,\frac{dX_s}{dT} - \left(\left.\frac{\partial C}{\partial X}\right|_{X=X_s} - \left.\frac{\partial C}{\partial X}\right|_{X=0}\right) = 0 \tag{14}$$

Substitutions of Eqs. 2 and 4 into Eq. 14, one arrives at after some rearrangement

$$\frac{d}{dT}\left[\left(\int_0^1 C\, d\eta - 1 - C_u\right)X_s\right] + \left.\frac{\partial C}{\partial X}\right|_{X=0} = 0 \tag{15}$$

In method III, integrodifferential equation proposed by Volkov and Li-Orlov[8] is used. One starts from double integration of Eq. 1 in the following manner:

$$\int_0^{X_s}\int_{X_s}^{X}\left(\frac{\partial C}{\partial T} - \frac{\partial^2 C}{\partial X'^2}\right) dX'\, dX = 0 \tag{16}$$

After integration, one has by using Eqs. 2–4

$$\int_0^{X_s}\int_{X_s}^{X}\frac{\partial C}{\partial T}\, dX'\, dX - \left(1 - C_u X_s \frac{dX_s}{dT}\right) = 0 \tag{17}$$

Upon applying Leibnitz's rule to the first term in Eq. 17, Eq. 17 becomes

$$\frac{d}{dT}\int_0^{X_s}\int_{X_s}^{X} C\, dX'\, dX + C(X_s, T)X_s\frac{dX_s}{dT} - \left(1 - C_u X_s\,\frac{dX_s}{dT}\right) = 0 \tag{18}$$

Substitution of Eq. 4 into Eq. 18, one arrives at after some rearrangement

$$\frac{d}{dT}\left[\left(\int_0^1\int_1^{\eta} C\, d\eta'\, d\eta + \frac{1}{2} + \frac{1}{2}C_u\right)X_s^2\right] - 1 = 0 \tag{19}$$

In calculations later, these three methods, based respectively on Eqs. 12, 15, and 19, are used for evaluating X_s with the help of Eq. 5. Comparing Eqs. 15 and 19, one can see that the derivative term is eliminated using double-integration technique as expressed by Eq. 16.

Approximate Polynomial Concentration Profiles

The most important approximation in integral methods is that concentration profiles are assumed to be one approximate concentration profile of single variable. For simplicity, approximate polynomial is used in usual. Approximate polynomial concentration profile does not satisfy original governing equation, that is, Eq. 1, however, it did satisfy integral equations. Approximate polynomial concentration profiles of different degree can be assumed, depending on boundary conditions or subsidiary conditions which they satisfy.[7] In addition to boundary conditions, that is, Eqs. 3 and 4, some subsidiary conditions can be derived by total differentiation technique. Differentiating Eq. 3 with respect to T, one has with the aid of Eq. 1

$$\left.\frac{\partial^2 C}{\partial X^2}\right|_{X=0} = 0 \tag{20}$$

Differentiating Eq. 4 with respect to T, one has by chain rule

$$\left.\frac{\partial C}{\partial T}\right|_{X=X_s} + \left.\frac{\partial C}{\partial X}\right|_{X=X_s}\frac{dX_s}{dT} = 0 \tag{21}$$

Upon substituting Eqs. 1 and 2 into Eq. 21, one arrives at

$$\left.\frac{\partial^2 C}{\partial X^2}\right|_{X=X_s} + \frac{1}{C_u}\left(\left.\frac{\partial C}{\partial X}\right|_{X=X_s}\right)^2 = 0 \tag{22}$$

Based on Eqs. 3 and 4, and using Eqs. 20 and 22 as auxiliary conditions, approximate polynomial concentration profiles of degree up to three at most as

$$C \cong a_3\eta^3 + a_2\eta^2 + a_1\eta + a_0 \tag{23}$$

can be derived, where a_3, a_2, a_1, and a_0 are coefficients. All possible polynomials are summarized as follows:

$$C \cong \eta \tag{24}$$

$$C \cong \left[-1 - C_u + \left(C_u^2 + 2C_u\right)^{1/2}\right]\eta^2 + \left[2 + C_u - \left(C_u^2 + 2C_u\right)^{1/2}\right]\eta \tag{25}$$

$$C \cong \frac{-2 - 3C_u + \left(9C_u^2 + 12C_u\right)^{1/2}}{4}\eta^3 + \frac{6 + 3C_u - \left(9C_u^2 + 12C_u\right)^{1/2}}{4}\eta \tag{26}$$

Here, linear polynomial as Eq. 24 satisfies Eqs. 3 and 4, quadratic polynomial as Eq. 25 satisfies Eqs. 3, 4, and 22, and cubic polynomial as Eq. 26 satisfies Eqs. 3, 4, 20, and 22.

Limits of these three polynomials for limiting cases of C_u can easily be evaluated. As C_u increases, upon applying L'Hospital's rule, limits for quadratic polynomial, cubic polynomial, and exact solution can be derived as follows:

$$\lim_{C_u\to\infty}\left\{\left[-1-C_u+\left(C_u^2+2C_u\right)^{1/2}\right]\eta^2+\left[2+C_u-\left(C_u^2+2C_u\right)^{1/2}\right]\eta\right\}$$
$$=\lim_{C_u\to\infty}\left\{\left[-\frac{1}{1+C_u+\left(C_u^2+2C_u\right)^{1/2}}\right]\eta^2+\left[1+\frac{1}{1+C_u+\left(C_u^2+2C_u\right)^{1/2}}\right]\eta\right\}=\eta \quad (27)$$

$$\lim_{C_u\to\infty}\left[\frac{-2-3C_u+\left(9C_u^2+12C_u\right)^{1/2}}{4}\eta^3+\frac{6+3C_u-\left(9C_u^2+12C_u\right)^{1/2}}{4}\eta\right]$$
$$=\lim_{C_u\to\infty}\left\{-\frac{1}{2+3C_u+\left(9C_u^2+12C_u\right)^{1/2}}\eta^3+\left[1+\frac{1}{2+3C_u+\left(9C_u^2+12C_u\right)^{1/2}}\right]\eta\right\}=\eta \quad (28)$$

$$\lim_{C_u\to\infty}\frac{\mathrm{erf}(\lambda\eta)}{\mathrm{erf}(\lambda)}=\lim_{\lambda\to 0}\frac{\mathrm{erf}(\lambda\eta)}{\mathrm{erf}(\lambda)}=\lim_{\lambda\to 0}\frac{e^{-\lambda^2\eta^2}\eta}{e^{-\lambda^2}}=\eta \quad (29)$$

Therefore, all of approximate polynomial concentration profiles approach to exact concentration profile as C_u increases. Similarly, when C_u approaches zero, limits of these polynomials can also be derived. The results are collected in Table 1.

For evaluation of approximate polynomial concentration profiles, an indicative parameter RC is defined as

$$\mathrm{RC}=\frac{\int_0^1(\text{Polynomial concentration profile})d\eta}{\int_0^1(\text{Exact concentration profile})d\eta} \quad (30)$$

Figure 2 demonstrates variations of RC for various values of C_u for these three polynomials. According to this figure, both results of linear polynomial and cubic polynomial show negative deviation from exact concentration profile, and approach to it steadily as C_u increases. However, that of quadratic polynomial shows dramatic change. The dash-curve increases from value lower than unity (negative deviation) to a maximum higher than unity (positive deviation) for smaller C_u, and then decreases to unity gradually for larger C_u. The positions of intersection between the dash-curve and line RC = 1, and maximum are indicated in figure caption. This dramatic change can be realized from concentration profiles as demonstrated in Figure 3. As C_u increases, before dash-curve intersects with line RC = 1, quadratic polynomial is below exact concentration profile for full range of η, as shown in Figure 3a, and hence RC is smaller than unity; after dash-curve intersects with line RC = 1, quadratic polynomial is above exact concentration profile for full range of η, as shown in Figure 3b, and hence RC is greater than unity. This figure also shows that both linear and cubic polynomials are always below exact concentration profile for full range of η. In the main, accuracy of quadratic polynomial is higher for smaller C_u, however, accuracy of cubic polynomial is higher for larger C_u. The demarcation is about at C_u = 0.50. The end behaviors of RC for these three polynomials when C_u is large can be realized by their limiting conditions, as discussed in the preceding context. The limits of RC for these three polynomials when C_u approaches zero are also collected in Table 1.

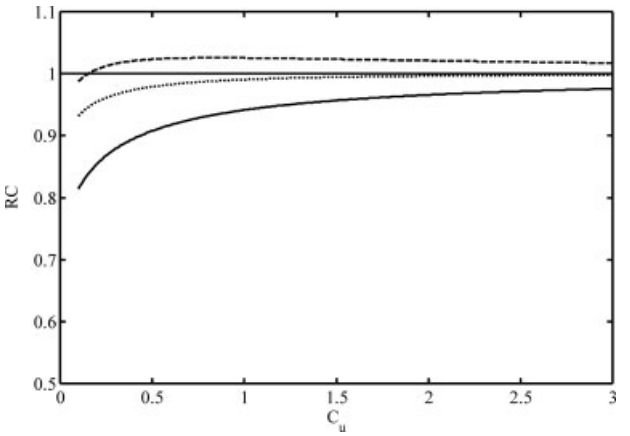

Figure 2. Variation of RC as a function of C_u for each polynomial concentration profile.

Solid curve, linear polynomial; dash-curve, quadratic polynomial; dot-curve, cubic polynomial. The dash-curve intersects with line RC = 1 at $C_u \cong 0.15$, and reaches maximum at $C_u \cong 0.84$.

Table 1. List of Limits of Concentrations Profiles and RC When $C_u \to 0$

	$\lim_{C_u\to 0} C$	$\lim_{C_u\to 0}$ RC
Exact	$\begin{cases}0, & \eta=0\\ 1, & \eta\neq 0\end{cases}$	
i (Linear polynomial)	η	$\frac{1}{2}$
ii (Quadratic polynomial)	$-\eta^2+2\eta$	$\frac{2}{3}$
iii (Cubic polynomial)	$-\frac{1}{2}\eta^3+\frac{3}{2}\eta$	$\frac{5}{8}$

Moving Saturation Front and Fraction of Drug Released

Upon substitution of approximate polynomial concentration profiles into Eqs. 12, 15, and 19, respectively, X_s can be solved subject to Eq. 5, and also f can be derived by using Eq. 10. There are nine groups of approximations in total, and which are collected in Tables 2 and 3, where in these two tables, roman numeral in capital denotes approximate method used, and that in lowercase denotes polynomial concentration

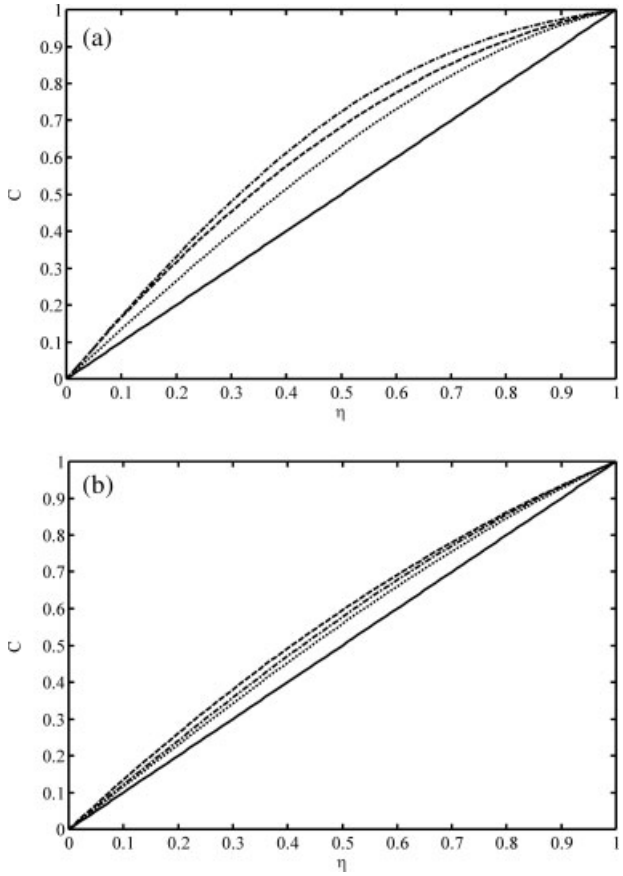

Figure 3. Variations of concentration profiles as a function of η when (a) $C_u = 0.05$ and (b) $C_u = 0.50$.

Dash-dot-curve, exact solution; solid curve, linear polynomial; dash-curve, quadratic polynomial; dot-curve, cubic polynomial.

Table 2. List of Approximations of X_s, Together with Exact Solution

	X_s	Equations Used
Exact	$2\lambda T^{1/2}$	
I-i	$\left(\frac{2}{C_u}\right)^{1/2} T^{1/2}$	(12) and (24)
I-ii	$\left[\frac{-2C_u+2\left(C_u^2+2C_u\right)^{1/2}}{C_u}\right]^{1/2} T^{1/2}$	(12) and (25)
I-iii	$\left[\frac{-3C_u+\left(9C_u^2+12C_u\right)^{1/2}}{C_u}\right]^{1/2} T^{1/2}$	(12) and (26)
II-i	$\frac{2}{(1+2C_u)^{1/2}} T^{1/2}$	(15) and (24)
II-ii	$\left[\frac{24+12C_u-12\left(C_u^2+2C_u\right)^{1/2}}{2+5C_u+\left(C_u^2+2C_u\right)^{1/2}}\right]^{1/2} T^{1/2}$	(15) and (25)
II-iii	$\left[\frac{48+24C_u-8\left(9C_u^2+12C_u\right)^{1/2}}{6+13C_u+\left(9C_u^2+12C_u\right)^{1/2}}\right]^{1/2} T^{1/2}$	(15) and (26)
III-i	$\left(\frac{6}{1+3C_u}\right)^{1/2} T^{1/2}$	(19) and (24)
III-ii	$\left[\frac{12}{1+5C_u+\left(C_u^2+2C_u\right)^{1/2}}\right]^{1/2} T^{1/2}$	(19) and (25)
III-iii	$\left[\frac{30}{3+12C_u+\left(9C_u^2+12C_u\right)^{1/2}}\right]^{1/2} T^{1/2}$	(19) and (26)

profile used. The pseudosteady state approximation suggested by Higuchi[3] is also included in these approximations, as indicated by II-i in these two tables. For evaluation of approximations, two indicative parameters, RX_s and Rf, are defined respectively as follows:

$$RX_s = \frac{\text{Approximation of } X_s}{\text{Exact solution of } X_s} \tag{31}$$

$$Rf = \frac{\text{Approximation of } f}{\text{Exact solution of } f} \tag{32}$$

Table 3. List of Approximations of f, Together with Exact Solution

	f	Equations Used
Exact	$\frac{2}{\pi^{1/2}(1+C_u)\mathrm{erf}(\lambda)} T^{1/2}$	
I-i	$\frac{1+2C_u}{2^{1/2}C_u^{1/2}(1+C_u)} T^{1/2}$	(12) and (24)
I-ii	$\frac{\left[2+5C_u+\left(C_u^2+2C_u\right)^{1/2}\right]}{6C_u^{1/2}(1+C_u)} \cdot \left[-2C_u+2\left(C_u^2+2C_u\right)^{1/2}\right]^{1/2} T^{1/2}$	(12) and (25)
I-iii	$\frac{\left[6+13C_u+\left(9C_u^2+12C_u\right)^{1/2}\right]}{16C_u^{1/2}(1+C_u)} \cdot \left[-3C_u+\left(9C_u^2+12C_u\right)^{1/2}\right]^{1/2} T^{1/2}$	(12) and (26)
II-i	$\frac{(1+2C_u)^{1/2}}{1+C_u} T^{1/2}$	(15) and (24)
II-ii	$\frac{\left[2+5C_u+\left(C_u^2+2C_u\right)^{1/2}\right]}{(1+C_u)\left[6+15C_u+3\left(C_u^2+2C_u\right)^{1/2}\right]^{1/2}} \cdot \left[2+C_u-\left(C_u^2+2C_u\right)^{1/2}\right]^{1/2} T^{1/2}$	(15) and (25)
II-iii	$\frac{\left[6+13C_u+\left(9C_u^2+12C_u\right)^{1/2}\right]}{(1+C_u)\left[192+416C_u+32\left(9C_u^2+12C_u\right)^{1/2}\right]^{1/2}} \cdot \left[6+3C_u-\left(9C_u^2+12C_u\right)^{1/2}\right]^{1/2} T^{1/2}$	(15) and (26)
III-i	$\frac{3+6C_u}{(1+C_u)(6+18C_u)^{1/2}} T^{1/2}$	(19) and (24)
III-ii	$\frac{2+5C_u+\left(C_u^2+2C_u\right)^{1/2}}{(1+C_u)\left[3+15C_u+3\left(C_u^2+2C_u\right)^{1/2}\right]^{1/2}} T^{1/2}$	(19) and (25)
III-iii	$\frac{30^{1/2}\left[6+13C_u+\left(9C_u^2+12C_u\right)^{1/2}\right]}{16(1+C_u)\left[3+12C_u+\left(9C_u^2+12C_u\right)^{1/2}\right]^{1/2}} T^{1/2}$	(19) and (26)

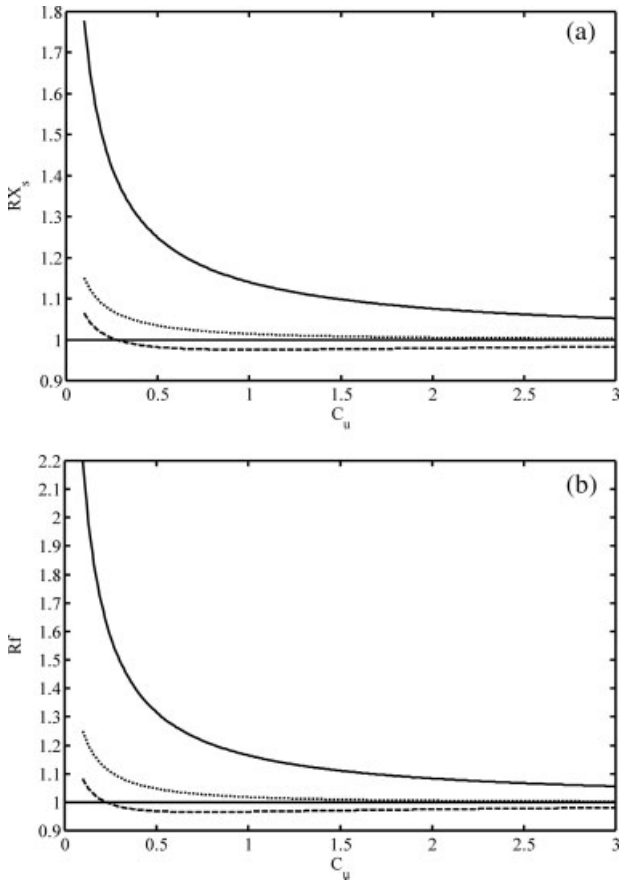

Figure 4. Variations of (a) RX_s and (b) Rf as a function of C_u by approximate method I using different polynomial concentration profiles.

Solid curves, I-i; dash-curves, I-ii; dot-curves, I-iii. In (a), the dash-curve intersects with line $RX_s = 1$ at $C_u \cong 0.28$, and reaches minimum at $C_u \cong 1.02$. In (b), the dash-curve intersects with line $Rf = 1$ at $C_u \cong 0.23$, and reaches minimum at $C_u \cong 0.75$.

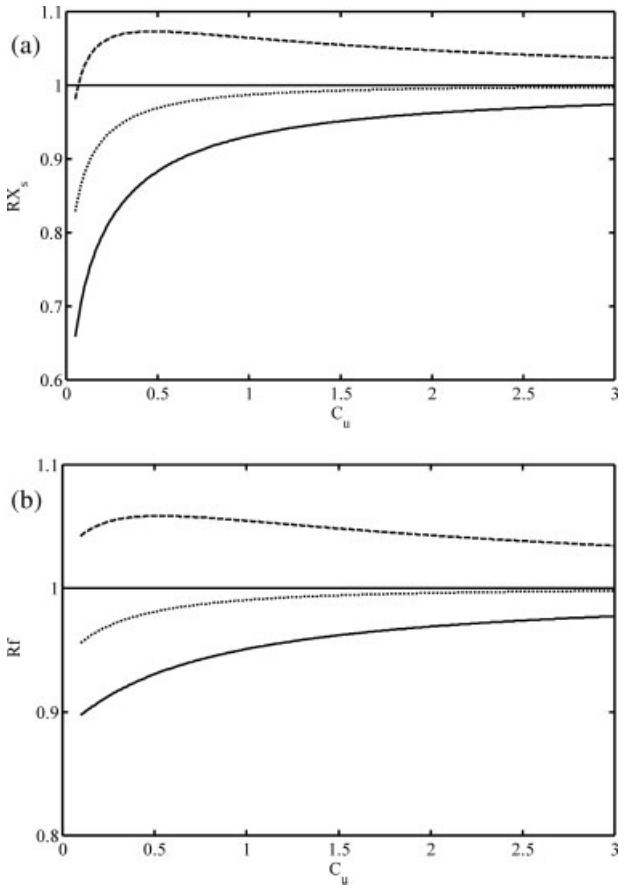

Figure 5. Variations of (a) RX_s and (b) Rf as a function of C_u by approximate method II using different polynomial concentration profiles.

Solid curves, II-i; dash-curves, II-ii; dot-curves, II-iii. In (a), the dash-curve intersects with line $RX_s = 1$ at $C_u \cong 0.07$, and reaches maximum at $C_u \cong 0.47$. In (b), the dash-curve reaches maximum at $C_u \cong 0.53$.

According to Tables 2 and 3, all of approximations, as well as exact solutions, are proportional to $T^{1/2}$; therefore, both of these two indicative parameters depend on the key parameter C_u only. Variations of RX_s and Rf for these three methods as C_u changes are demonstrated in Figures 4–6, respectively. At first sight, the results seem to be irregular. However, if one refers to results of RC, depicted in Figure 2, some global regularities can be concluded. In the main, all of these approximations vary roughly corresponding to variations of RC. First, all of these approximations approach to exact solutions when C_u is large. This is easily realized by the end behaviors of approximate polynomials and exact concentration profiles, as mentioned in the fourth section. The limits of RX_s and Rf for these approximations when C_u approaches zero are collected in Table 4. Second, both results applying linear polynomial and cubic polynomial, regardless of the methods, appear negative/positive deviation, and increase/decrease steadily to unity when C_u increases. However, that applying quadratic polynomial appears increasing followed decreasing, or decreasing followed increasing, demarcated by extremum point. The positions of intersections and extremum points are indicated in the captions of these figures. Third, for each method, accuracy of result applying cubic polynomial is higher when C_u is larger than about 1.00. However, in the vicinity of intersection between dash-curve and $RX_s = 1$ (or $Rf = 1$ for figures of Rf), that applying quadratic polynomial seems to be higher. Notice that positions of intersections for RX_s and Rf are not the same. For general applications, C_u is not too small, and

Table 4. List of Limits of Both RX_s and Rf of Each Approximation When $C_u \to 0$

	$\lim_{C_u \to 0} RX_s$	$\lim_{C_u \to 0} Rf$
I-i	∞	∞
I-ii	∞	∞
I-iii	∞	∞
II-i	0	$\left(\frac{\pi}{4}\right)^{1/2}$
II-ii	0	$\left(\frac{\pi}{3}\right)^{1/2}$
II-iii	0	$\left(\frac{9\pi}{32}\right)^{1/2}$
III-i	0	$\left(\frac{3\pi}{8}\right)^{1/2}$
III-ii	0	$\left(\frac{\pi}{3}\right)^{1/2}$
III-iii	0	$\left(\frac{45\pi}{128}\right)^{1/2}$

therefore cubic polynomial is the most appropriate. The results (*Rf*) applying cubic polynomial for these three methods are demonstrated in Figure 7. As this figure shows, the result is the most satisfactory if method III is used.

Conclusion

In this contribution, considering release of drug dispersed excessively in polymer matrix, applicability of three kinds of approximate methods, including two integral methods, are analyzed when polynomial concentration profiles of degree up to three are introduced. There are several points concluded from the results:

(1) Accuracy of results is dominated by accuracy of polynomial concentration profile.

(2) For general applications, integral method suggested by Volkov and Li-Orlov[8] is the most satisfactory if cubic polynomial concentration profile is introduced.

(3) For conditions in which excess quantity of drug in polymer matrix is small, quadratic polynomial concentration profile may be more adequate than cubic one.

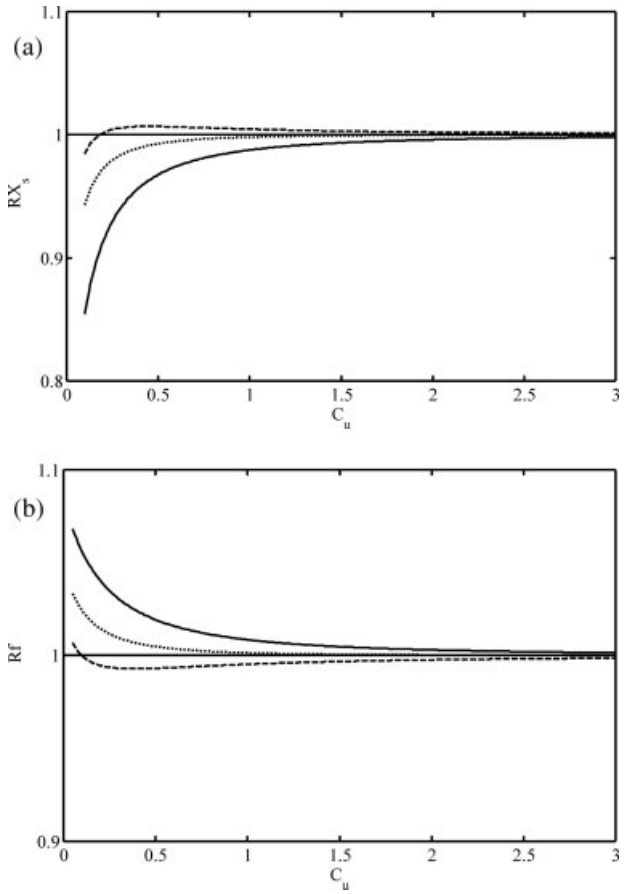

Figure 6. Variations of (a) RX_s and (b) *Rf* as a function of C_u by approximate method III using different polynomial concentration profiles.

Solid curves, III-i; dash-curves, III-ii; dot-curves, III-iii. In (a), the dash-curve intersects with line $RX_s = 1$ at $C_u \cong 0.18$, and reaches maximum at $C_u \cong 0.45$. In (b), the dash-curve intersects with line $Rf = 1$ at $C_u \cong 0.10$, and reaches minimum at $C_u \cong 0.38$.

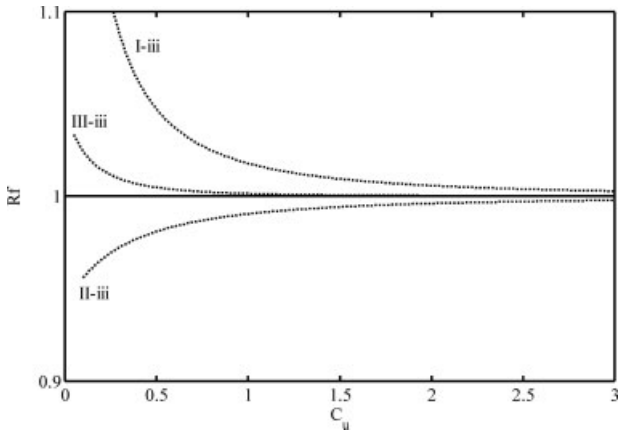

Figure 7. Variations of *Rf* as a function of C_u by different approximate methods using cubic polynomial concentration profile.

Acknowledgments

This work is supported by the National Science Council of the Republic of China.

Notation

a_i = coefficients of approximate polynomial concentration profile
c = concentration of drug in diffusion zone
c_s = solubility of drug in polymer matrix
c_u = quantity of undissolved drug per unit volume
$C = c/c_s$
$C_u = c_u/c_s$
D = diffusivity of drug in polymer matrix
f = fraction of drug released
l_p = half thickness of polymer matrix
RC = indicative parameter defined in Eq. 30
Rf = indicative parameter defined in Eq. 32
RX_s = indicative parameter defined in Eq. 31
t = time
$T = Dt/l_p^2$
x = abscissa of coordinate
x_s = position of moving saturation front
$X = x/l_p$
$X_s = X_s/l_p$

Greek letters

$\eta = x/x_s = X/X_s$
λ = parameter determined by C_u

Literature Cited

1. Carslaw HS, Jaeger JC. *Conduction of Heat in Solids*, 2nd ed. Oxford: Oxford University Press, 1959.
2. Paul DR, McSpadden SK. Diffusional release of a solute from a polymer matrix. *J Membr Sci*. 1976;1:33–48.
3. Higuchi T. Rate of release of medicaments from ointment bases containing drugs in suspension. *J Pharm Sci*. 1961;50:874–875.
4. Goodman TR. The heat-balance integral and its application to problems involving a change of phase. *Trans ASME*. 1958;80:335–342.
5. Goodman TR. The heat-balance integral-further considerations and refinements. *J Heat Transfer*. 1961;83:83–86.
6. Goodman TR. Application of integral methods to transient nonlinear heat transfer. In: Irvin TF, Hartnett JP, editors. *Advances in Heat Transfer, Vol. 1*. New York: Academic Press, 1964:51–122.
7. Langford D. The heat balance integral method. *Int J Heat Mass Transfer*. 1973;16:2424–2428.

8. Volkov VN, Li-Orlov VK. A refinement of the integral method in solving the heat conduction equation. *Heat Transfer Sov Res*. 1970;2:41–47.
9. Lee PI. Diffusional release of a solute from a polymeric matrix - approximate analytical solutions. *J Membr Sci*. 1980;7:255–276.
10. Selim MS, Seagrave RC. Solution of moving-boundary transport problems in finite media by integral transforms. I. Problems with a plane moving boundary. *Ind Eng Chem Fundam*. 1973;12: 1–8.
11. Longwell PA. A graphical method of solution of freezing problems. *AIChE J*. 1958;4:53–57.
12. Landau HG. Heat conduction in a melting solid. *Q Appl Math*. 1950;8:81–94.
13. Crank J. *The Mathematics of Diffusion*, 2nd ed., reprinted in paperback. New York: Oxford University Press, 1992.
14. Wu XY, Zhou Y. Studies of diffusional release of a dispersed solute from polymeric matrixes by finite element method. *J Pharm Sci*. 1999;88:1050–1057.
15. Schlichting H, Gersten K. *Boundary-Layer Theory*, *8th revised and enlarged edition*, with contributions from Krause E, Oertel H, Jr., translated by Mayes K. Berlin: Springer, 2000.

Manuscript received Jun. 15, 2007, revision received Feb. 20, 2008. and final revision received Apr. 29, 2008